

JOINT INSTITUTE FOR NUCLEAR RESEARCH
Veksler and Baldin Laboratory of High Energy Physics

FINAL REPORT ON THE START PROGRAMME
Construction of correlation function for pions from $Au+Au$ collisions at
 $\sqrt{s_{NN}} = 200 \text{ GeV}$ STAR experiment

Supervisor: Artem Korobitsin
Student: Siranush Asatryan
Armenia, Yerevan State University
Participation period: 07 August – 17 September

Dubna, 2022

Abstract

Femtoscopic measurements of two-particle correlations at small relative momenta provide means to study space-time extents of system created in high-energy heavy-ion collisions. The size of particle in these collisions can be deduced. Such correlations arise due to quantum statistics and Coulomb and strong final state interactions. In this work, results are presented from femtoscopic analyses of $\pi^+\pi^+$ correlations from $Au+Au$ collisions at $\sqrt{S_{NN}}=200$ GeV STAR experiment at the RHIC. One-dimensional correlation functions of the system are constructed for different centralities and k_T bins in terms of the invariant momentum difference of the pair.

Table of Contents

1. Introduction	
1.1 The STAR experiment.....	4
1.2 Time Projection Chamber.....	4
1.3 Time of Flight detector.....	6
2. Femtoscopy	
2.1 Two-particle correlation function.....	7
2.2 Correlation function construction.....	8
3. Data analysis	
3.1 Event selection.....	8
3.2 Particle selection.....	10
3.3 k_T cuts.....	12
3.4 Correlated two-particle distributions.....	13
4. Results	
4.1 One-dimensional correlation functions.....	14
Conclusion.....	15
Bibliography.....	16

1. Introduction

1.1 The STAR experiment

The Relativistic Heavy Ion Collider (RHIC) located at Brookhaven National Laboratory (BNL) in Upton, New York, is the second most powerful heavy-ion collider in the world. The primary goal of the physics program at RHIC is to produce and to study a deconfined state of nuclear matter, Quark-gluon Plasma (QGP) by the high-energy heavy-ion collisions.

RHIC has the capability to accelerate a variety of particle species to ultra-relativistic speed and since its commission in 2000, RHIC has successfully collided $Au + Au$, $p + Au$, $d + Au$, $^3He + Au$, $Cu + Au$, $Cu + Cu$, $U + U$, $p + Al$ and $p + p$. In particular, the most important for the study of phase-space diagram of nuclear matter is the RHIC's capability to accelerate and collide ions at different energies.

The Solenoid Tracker At the RHIC (STAR) is a multi-purpose detector designed to investigate the behavior of strongly interacting matter at high energy density and to search for signatures of QGP formation. Figure 1.1 shows schematic picture of the STAR detector. As can be seen, STAR detector contains various subsystems.

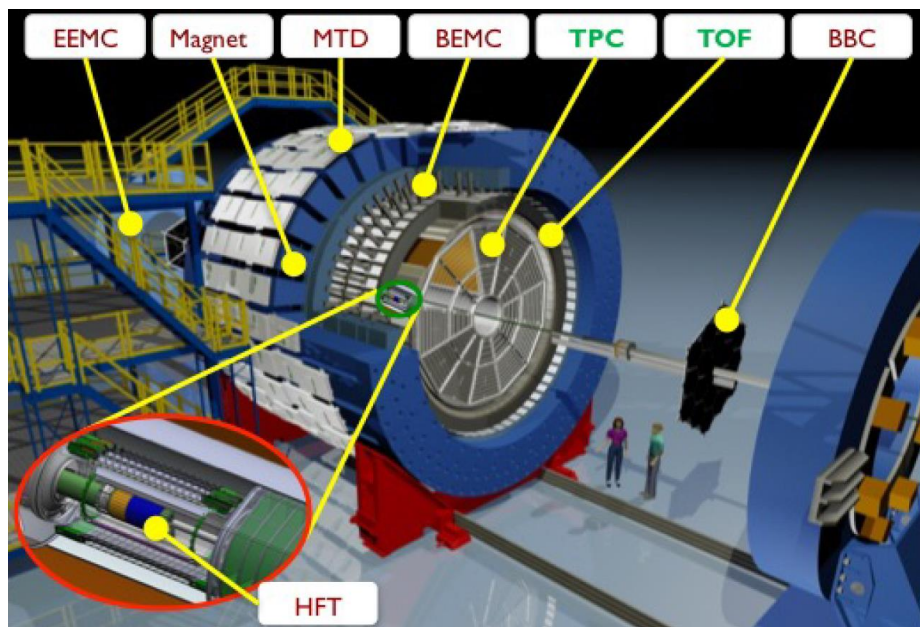


Figure 1.1: STAR detector with a cutaway for viewing the inner detectors [1]

1.2 Time Projection Chamber

The heart of the STAR detector is the Time Projection Chamber (TPC), which is surrounded by the Time-of-Flight detector (ToF) and the Barrel Electromagnetic Calorimeter (BEMC). There are also forward detectors, such as the Beam-Beam Counter (BBC) and the Endcap Electromagnetic Calorimeter (EEMC). The central subsystems sit in the STAR magnet, which has an outer radius

of 3.66 m and a length of 6.85m and is capable to produce a uniform magnetic field of 0.5 T along the beam axis.

The TPC, 4.2 m long cylinder with 4 m in diameter, is the primary tracking detector in the STAR. It is used to reconstruct the trajectory of charged particles in three dimensions and measures momentum. TPC is filled with gas. When charged particle crosses through the gas, it ionizes it. TPC also has a cathode end and a segmented anode end which is connected to the readout system. This imposes field lines on the volume of the cylinder so that the ionized electrons drift to one side and the positive ions to the other. As the anode plate is segmented, the pad where the electron falls is recorded and this gives the X and Y position of the particle trajectory. Knowing the drift time of electrons in a specific gas and the external trigger which gives information about arrival of a particle, we can get the Z position of the track. Thus, the track can be fully reconstructed in three dimensions. The position of hits from the pads are used for the tracking. Tracks are reconstructed by extrapolating along the approximate direction of the hitting points. Figure 1.2 shows reconstructed $Au+Au$ collisions at $\sqrt{s_{NN}} = 200 \text{ GeV}$, recorded by the STAR detector. The blue lines represent measured tracks by the TPC.

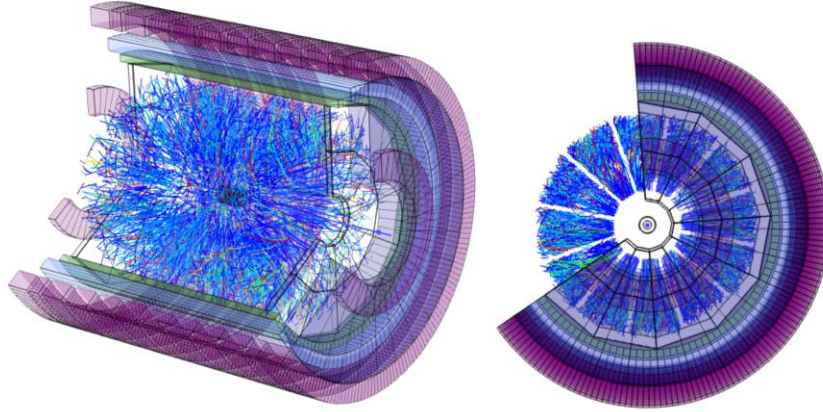


Figure 1.2: The trajectories of particles, which was reconstructed from TPC [2]

The particle identification is based on measurement of the dE/dx ionization energy loss in the TPC gas. The energy loss for charged particles as a function of momentum is shown in Figure 1.3. Energy loss is mass ordered, which means that heavier particles lose more energy in comparison to the lighter for the same momentum. STAR is able to separate pions, kaons and protons with a very good accuracy up to $1.2 \text{ GeV}/c$. Energy loss of charged particles by ionization, mentioned above, can be calculated using the Bethe-Bloch formula

$$-\left\langle \frac{dE}{dx} \right\rangle = 2\pi N_A r^2 m c^2 \rho \frac{Z}{A} \frac{z^2}{\beta^2} \left[\ln\left(\frac{2mc^2 \beta^2 W_{Max}}{I^2}\right) - \beta^2 - \frac{\delta^2}{2} \right] \quad (1)$$

where N_A is Avogadro's number, r is classical radius, m is mass of particle, c is speed of light in vacuum, ρ is density of the material, Z and A are atomic number and weight of material, W_{Max} is maximum energy transfer in a single collision, I is mean excitation energy and δ is density correction.

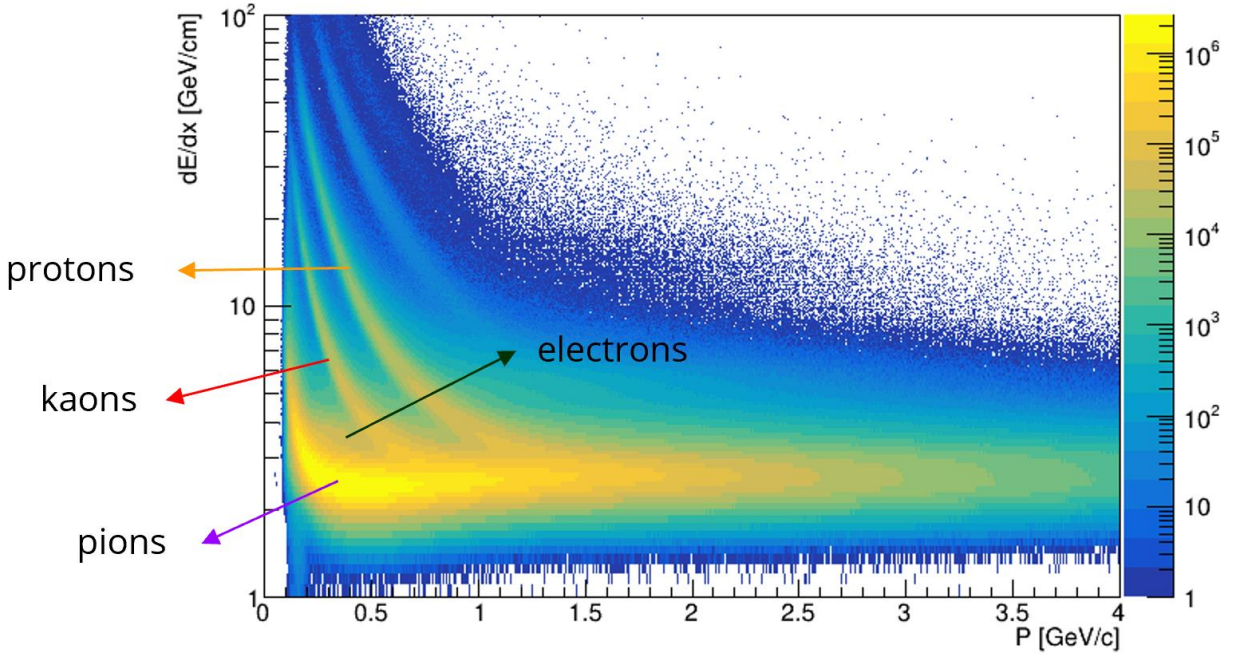


Figure 1.3: The TPC dE/dx versus total momentum p distribution. Pions, kaons, protons and electrons are identified.

1.3 Time of Flight detector

TPC has a problem to identify the charged hadrons such as π and K , if their momentum is above $\sim 0.7 \text{ GeV}/c$. The ToF was developed to improve particle identification. Figure 1.4 shows, that the ToF provides very good identification of charged pions, kaons, protons and electrons. TOF determines charged particle velocity by measuring the time required to travel from the interaction point to the time-of-flight detector. The system consists of two separate detector subsystems, start detector and stop detector. The electronic signals from these detectors define the time intervals of interest for particle Time of Flight measurements. The start detector consists of two identical detector assemblies that are positioned very close to the beam pipe and outside the STAR magnet. The end detector sits inside the STAR magnet immediately outside the TPC. The signals from these detectors are carried to electronics racks for digitization and interfacing with the STAR data stream.

$stop \text{ time} - start \text{ time} \equiv \tau$ (time of flight) is associated with reconstructed tracks in the TPC by track extrapolation to the TOF detectors. The TPC detector provides the momentum p , and total length L , so we can calculate inverse velocity [3]

$$\frac{1}{\beta} = \frac{c\tau}{L}$$

where c is speed of light. From the relativistic particle momentum, we obtain

$$p = m\beta\gamma \Rightarrow p^2 = \beta^2(m^2 + p^2)$$

where m is particle mass, one can derive the relation between β and p and get the particle mass squared

$$\frac{1}{\beta} = \sqrt{\left(\frac{m^2}{p^2} + 1\right)} \quad (2)$$

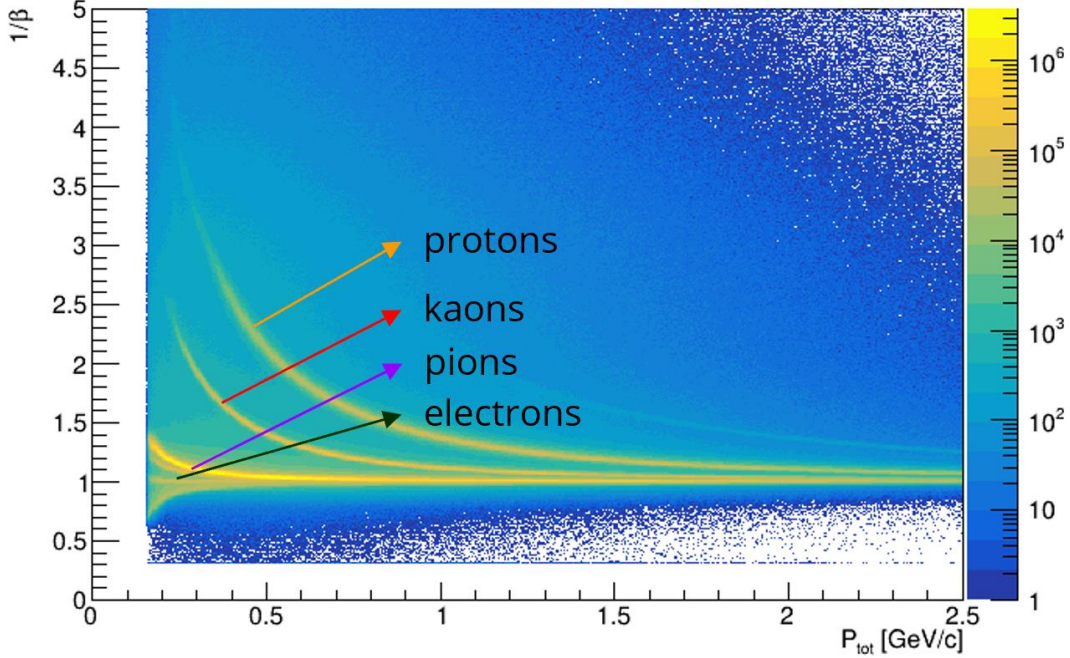


Figure 1.4: The ToF $1/\beta$ versus total momentum p

2. Femtoscopy

Technique called femtoscopy is developed for measurement of sizes and form of objects of order of 1 fm (1 femtometer). This method is based on studying of the correlation of identical particles shooting out from the interaction area and having small relative speeds or momentum.

2.1 Two-particle correlation function

For noninteracting identical particles, like pions, correlations result from the interference of the production amplitudes due to the symmetrization requirement of quantum statistics, also from Coulomb interaction. In practice, the correlation of two particles, a and b for a given pair momentum \mathbf{P} and relative momentum \mathbf{q} , is nominally given by

$$C_{\mathbf{P}}^{ab}(\mathbf{q}) = \frac{A_{\mathbf{P}}^{ab}(\mathbf{q})}{B_{\mathbf{P}}^{ab}(\mathbf{q})} \cdot \xi_{\mathbf{P}}(\mathbf{q}), \quad (3)$$

where $A_p^{ab}(\mathbf{q})$ is the signal distribution, $B_p^{ab}(\mathbf{q})$ is the reference or background distribution which is ideally similar to A in all respects except for the presence of femtoscopic correlations, and $\xi_p(\mathbf{q})$ is a correction factor introduced to compensate for non-femtoscopic correlations present in the signal that are not fully accounted for in the background as well as artifacts resulting, e.g., from finite resolution and contamination. If particles fly out independently of each other, $C(q)$ will be equal to 1. If the particles are not independent, they interact and are correlated, $C(q)$ won't be equal to 1.

2.2 Correlation function construction

Experimentally, the two-particle correlation function between identical particles is obtained from the ratio

$$C(\vec{q}, \vec{k}) = \frac{A(\vec{q})}{B(\vec{q})}, \quad (4)$$

where $A(\mathbf{q})$ is the pair distribution with relative momentum \mathbf{q} in the same event (real pairs), while $B(\mathbf{q})$ is the pair distribution with relative momentum \mathbf{q} in the different events (mixed pairs). Mixed pairs are made by event mixing technique.

3. Data analysis

In this work, femtoscopy correlation of positive charged pions was presented. Dataset was taken from $Au+Au$ collisions at $\sqrt{s_{NN}} = 200 \text{ GeV}$ by the STAR experiment at RHIC. Total number of events was used is 7.8 million. This chapter will present methods that were used to analyze the data.

3.1 Event selection

For the analysis, selection of events in the center of the TPC is required, to avoid events that haven't occurred in the center of the TPC. For that purpose, a cut on the position of the primary vertex along the beam direction (z-axis) was applied. Events required to have a cut of $|V_z| < 35 \text{ cm}$, where V_z is the z-coordinate of the primary vertex position which is measured by the TPC (see Figure 3.1). Tails of the histogram for primary vertex in z-direction do not contain enough counts and therefore they are not added into analysis. For the same purpose, such event cuts on x and y coordinate of primary vertex position were also applied (see Figure 3.2).

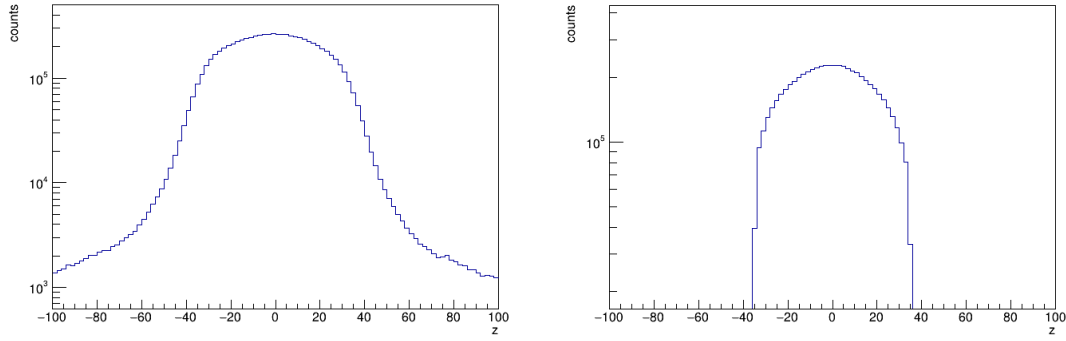


Figure 3.1: Event cuts on primary vertex in Z direction

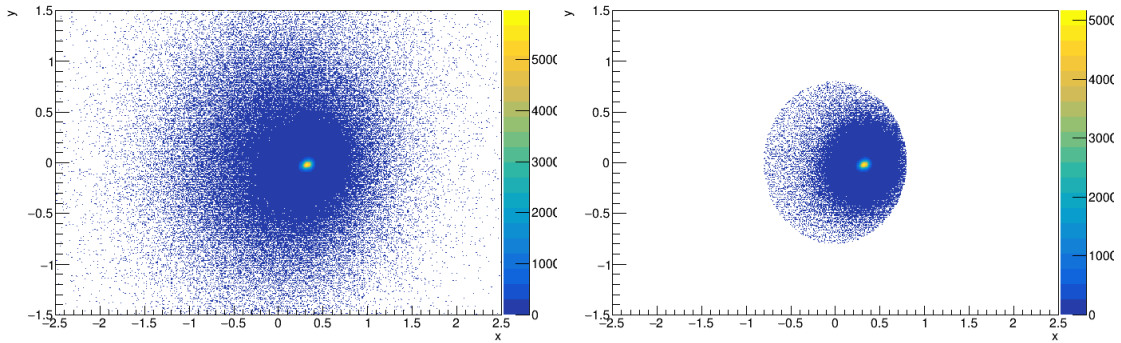


Figure 3.2: Event cut of $\sqrt{x^2 + y^2} < 0.8 \text{ cm}$ on primary vertex in x and y directions

The centrality of the collision was characterized according to measured multiplicity of the charged particles, i.e., the average number of charged particles, produced in a collision at a given energy in the center of mass system. For the analysis presented in this work, events were divided into 3 bins of centrality, corresponding to 0-20%, 20-50% and 50-80%, as shown on Figure 3.3.

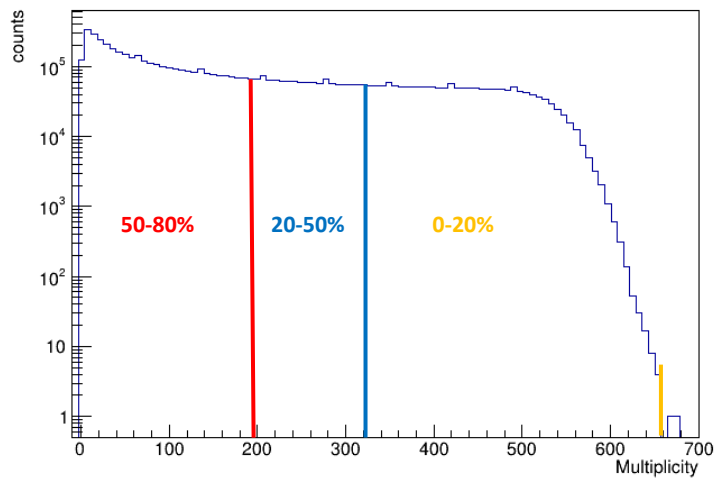


Figure 3.3: Multiplicity distribution with corresponding centrality

3.2 Particle selection

After selecting events, desired particles should be selected. As described in Chapter 1, particle identification is done in the TPC and ToF detectors. To make sure, that measured particles fall into detector acceptance, only tracks with pseudorapidity $|\eta| < 1.0$ were accepted. Resulting tracks are denoted as global tracks and determine the vertex primary position. Tracks were required to have the distance of closest approach (DCA) to the primary vertex smaller than 2 cm. These tracks are called primary tracks. DCA cuts are shown on Figure 3.4.

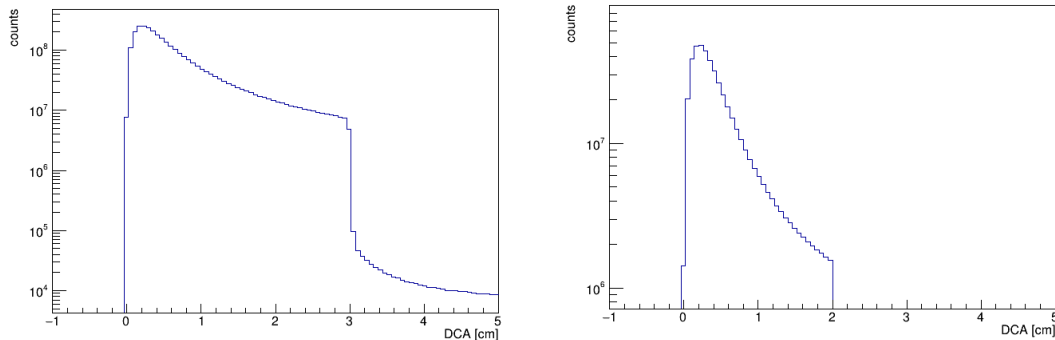


Figure 3.4: DCA distribution without (on the left) and with (on the right) cut

Another cut for track quality selection is based on the minimal number of reconstructed hits in TPC and criterion on the ratio of fitted hits to maximum possible number of hit points. The purpose of these quality cuts is to reduce effects such as track merging or imprecisely reconstructed tracks. Maximum possible number of hits of one track can leave in TPC is 45, as you can see on Figure 3.5. However, in practice, this value is smaller, since the maximum of hits depends on the transverse momentum and pseudorapidity of the track as well as on the detector effects. Track were required to have minimal 15 fit points in TPC and the ratio of fitted hits to maximal possible hits in TPC was more than 0.52.

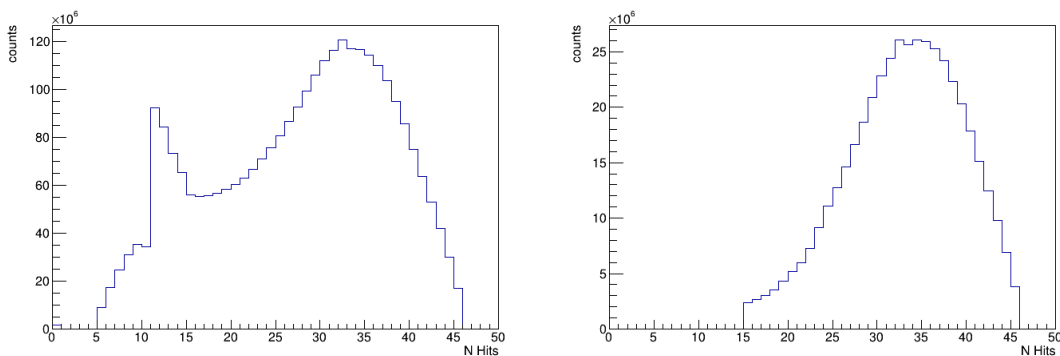


Figure 3.5: Number of hits distribution without (on the left) and with (on the right) cut

After tracks that passed those quality cuts, pion tracks should be selected. Since the TPC enables to identify particles with the transverse momentum p_T larger than $0.15 \text{ GeV}/c$, in addition a cut on the transverse momenta of the reconstructed tracks was applied. Only tracks with $p_T < 1.55 \text{ GeV}/c$ were identified as pions. Cuts for total and transverse momentum are shown in Figure 3.6.

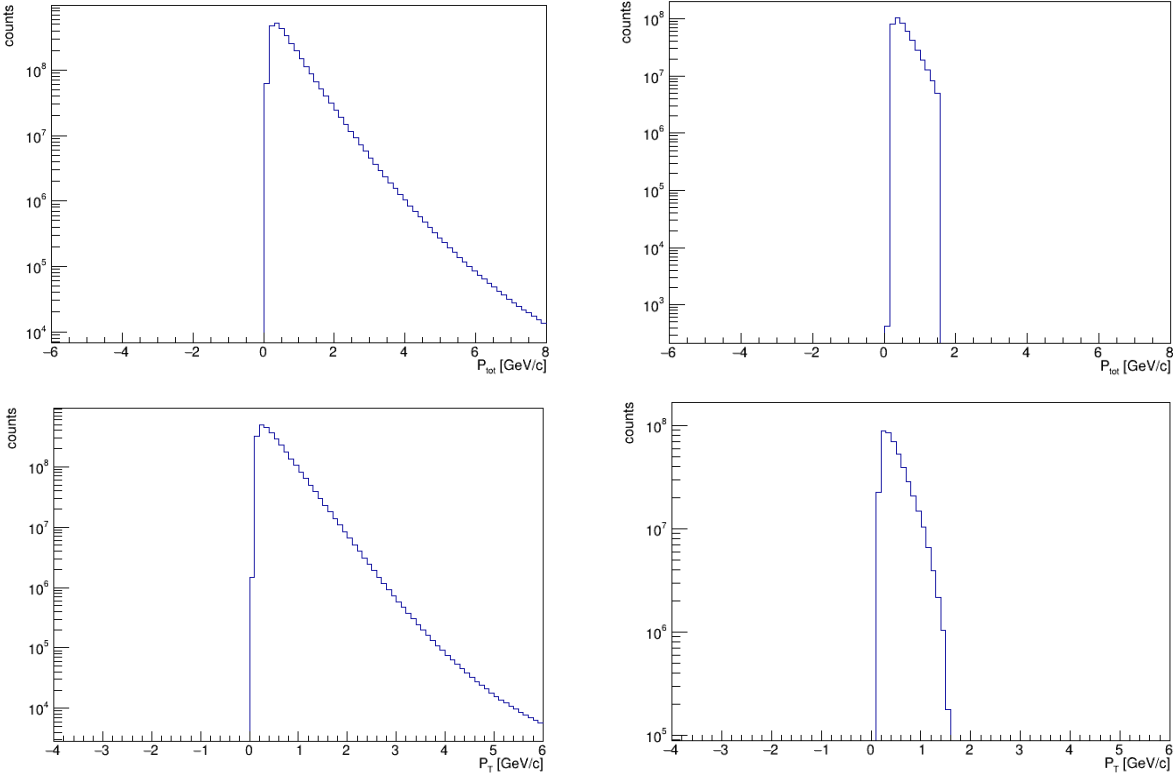


Figure 3.6: Before and after cuts on total (first row) and transverse (second row) momentum

After all these cuts are applied, pions should be selected by putting cut on pion's standard deviation, limiting it by $|\sigma_{pion}| \leq 2$ (see Figure 3.7).

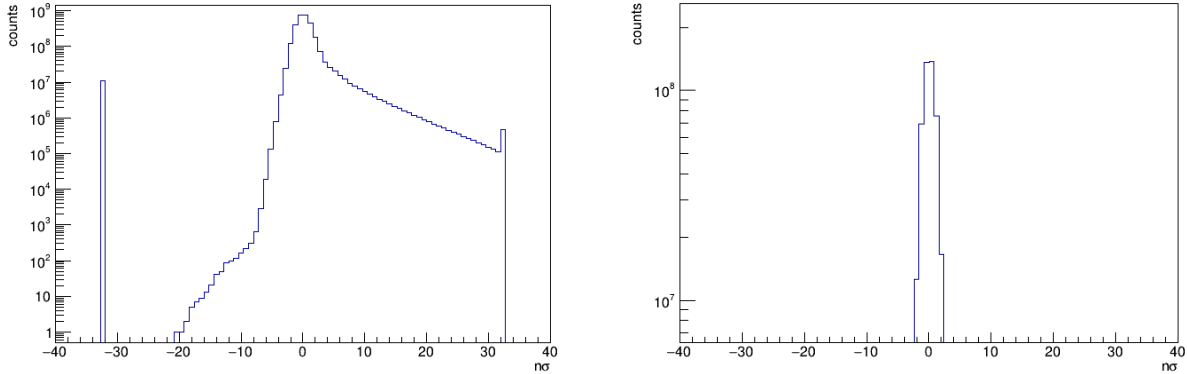


Figure 3.7: Pion standard deviation without (on the right) and with (on the left) cuts

But, as we can see in Figure 1.3, part of the pion distribution is overlapped by electron distribution. In order to remove it, ToF cut had to be used. The ToF measures the relative particle speed β . When this information is combined with the measured momentum in TPC, the particle mass m can be calculated by the following equation

$$m^2 = p^2 \left(\frac{1}{\beta^2} - 1 \right) \quad (5)$$

Since for pions $m_p^2 = 0.019 \text{ GeV}^2/c^4$, identification cut requires the track to have the mass squared in the range $-0.02 < m^2 < 0.062$. Figure 3.8 shows pion identification cut for ToF detector.

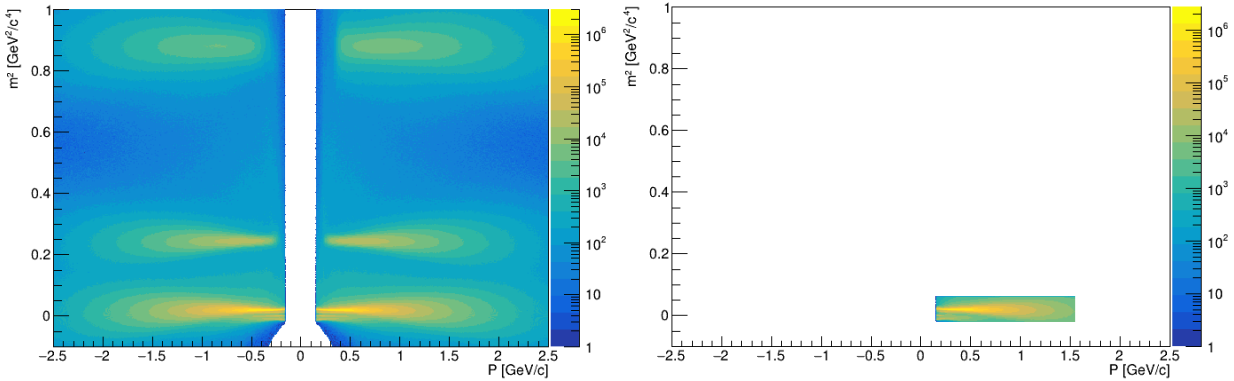


Figure 3.8: Pion identification on ToF. Without cut (on the right) and with cut (on the left)

After all these cuts, pion distribution is clearly visible on TPC dE/dx versus p distribution (see Figure 3.9).

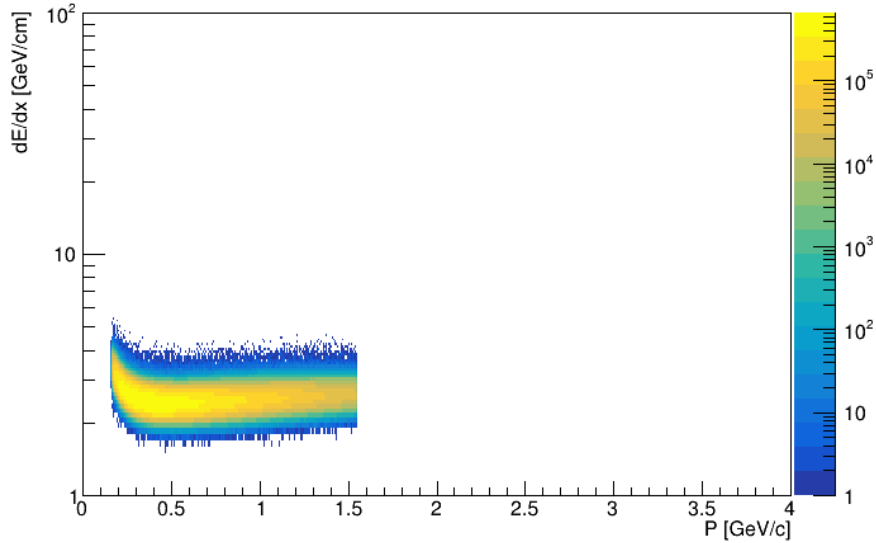


Figure 3.9: TPC dE/dx versus p distribution for pions

3.3 k_T cuts

Finally, the last applied cut is on the average pair transverse momentum k_T defined as

$$k_T = \left(\frac{\mathbf{p}_1 + \mathbf{p}_2}{2} \right)_T, \quad (6)$$

where \mathbf{p}_1 and \mathbf{p}_2 are the momenta of the first and second particle in the given pair. such cut enables to change the size of the measured volume at the constant centrality of the system. The average transverse momentum can be rewritten in the term of the transverse mass, which is suitable for the study of the m_T dependence of the correlation function.

The pairs were required to have the average transverse momenta in the range from 0.05 GeV/c to 1.25 GeV/c. This range was consequently divided into three bins: 0.05-0.45, 0.45-0.85 and 0.85-1.25 GeV/c. Figure 3.9 shows the k_T distribution of real like-sign pion pairs.

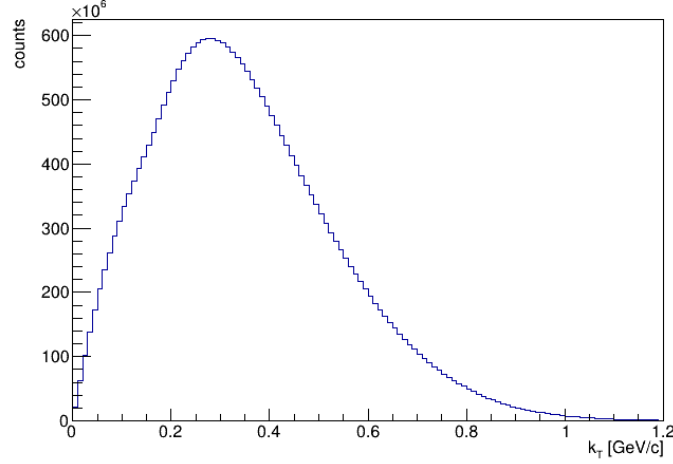


Figure 3.10: The distribution of real pair transverse momentum.

3.4 Correlated two-particle distributions

The simplest correlation function is constructed only in one dimension as a function of q_{inv} which is defined

$$q_{inv} = \sqrt{(E_1 - E_2)^2 - (\mathbf{p}_1 - \mathbf{p}_2)^2}. \quad (7)$$

This correlation function $CF(q_{inv})$ can be constructed as a ratio of the correlated two-particle distribution from the same event, $N_{same}(q_{inv})$ and the uncorrelated two-particle distribution from mixed events, $N_{mixed}(q_{inv})$ by the formula (4). These distributions are shown on Figure 3.11.

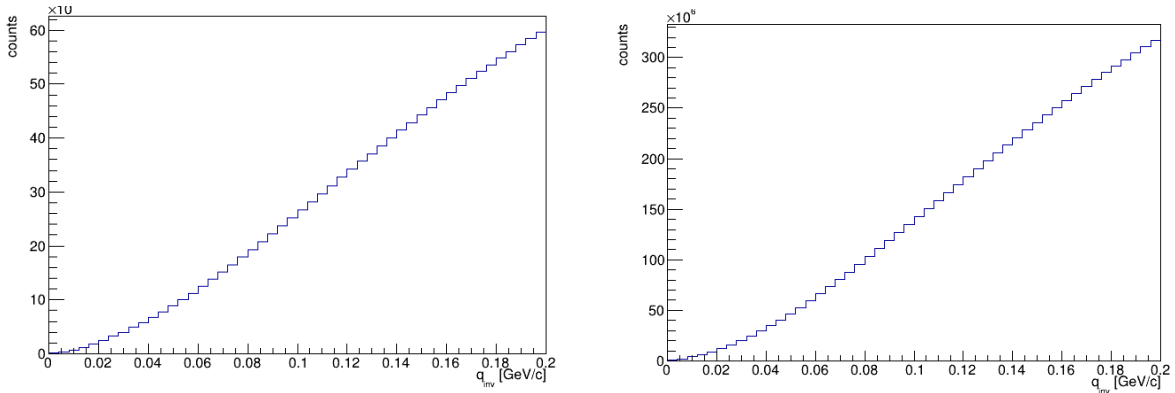


Figure 3.11: left: pair distribution with relative momentum q in the same event (real pairs), right: pair distribution with relative momentum q in the different events (mixed pairs)

4. Results

4.1 One-dimensional correlation functions

Figure 4.1 and 4.2 presents results on the positive charged pions correlation function from $Au+Au$ collisions at $\sqrt{s_{NN}} = 200$ GeV. Centrality dependence of positive charged pions correlation functions, which are integrated over k_T is shown in the Figure 4.1.

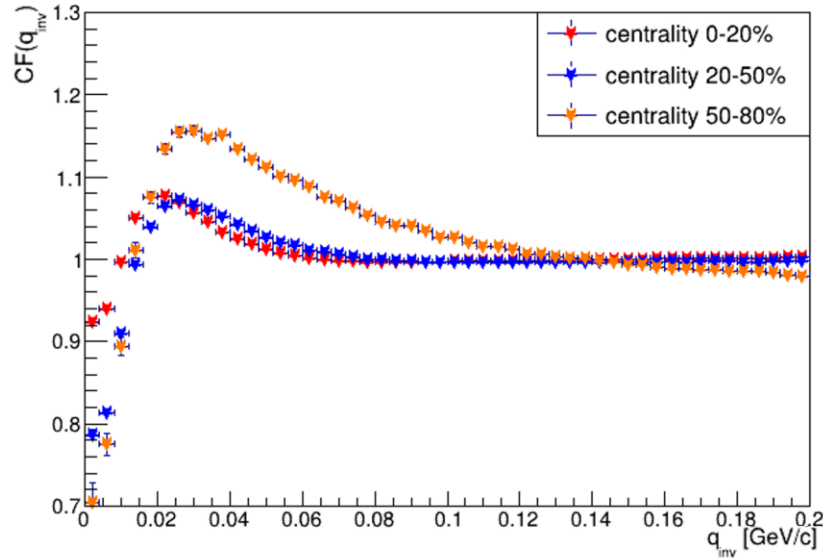
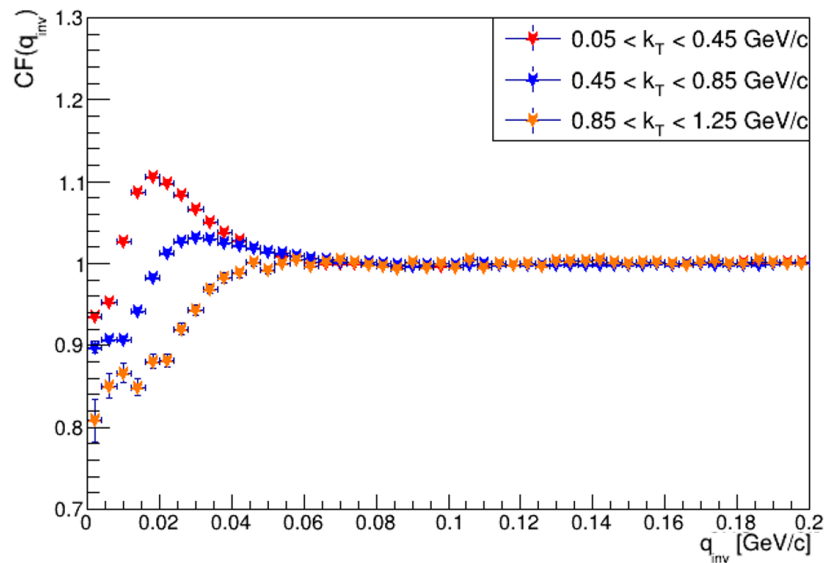


Figure 4.1: One dimensional positive charged pions correlation functions for 3 centralities.

Figure 4.2 presents like-sign correlations for 3 k_T bins and 2 centralities.



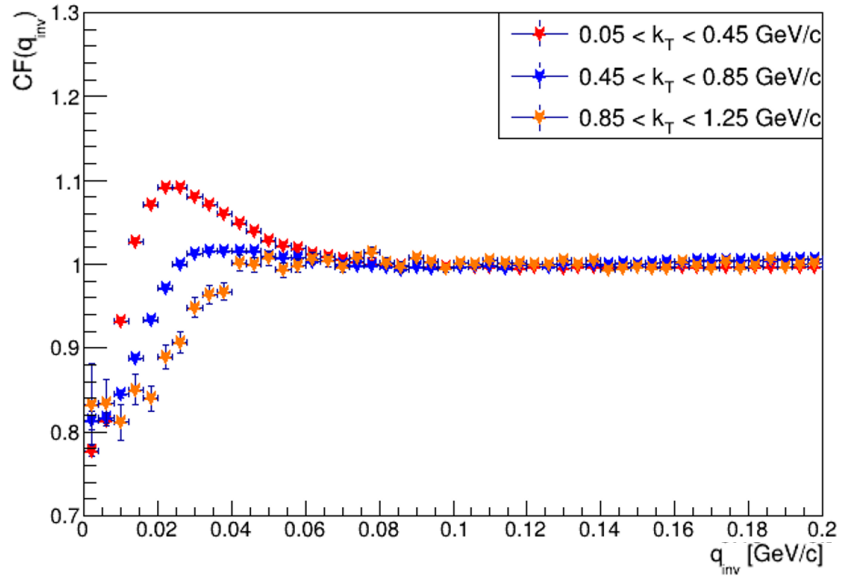


Figure 4.2: Top: One dimensional like-sign correlation functions for centrality 0-20% and for 3 k_T bins. Bottom: One dimensional like-sign correlation functions for centrality 20-50% and for 3 k_T bins.

Conclusion

In this work, femtoscopic study of two-particle correlation function for positive charged pions was done. The presented analysis was performed on data from $Au+Au$ collisions at $\sqrt{s_{NN}} = 200$ GeV collected by the TPC and ToF detectors of STAR experiment. Then, the one-dimensional correlation functions for pairs of positive pions were constructed (see Figure 4.1, 4.2). Functions were constructed for three centrality and three k_T bins. As can be seen, correlation of two particles decreases with increasing k_T . In furthermore analysis two-particle effects should be taken into consideration.

Bibliography

- [1] Brookhaven National Laboratory. Laboratory, <http://www.star.bnl.gov>
- [2] Brookhaven National Laboratory. Laboratory, <http://www.star.bnl.gov>
- [3] Proposal for a Large Area Time of Flight System for STAR.
https://www.star.bnl.gov/public/tof/publications/TOF_20040524.pdf.